Neural network microwave precipitation retrievals and modeling results

Citation: Leslie, R. Vincent et al. "Neural network microwave precipitation retrievals and modeling results." Microwave Remote Sensing of the Atmosphere and Environment VI. Ed. Azita Valinia, Peter H. Hildebrand, & Seiho Uratsuka. Noumea, New Caledonia: SPIE, 2008. 715406-8.

As Published: http://dx.doi.org/10.1117/12.804815

Publisher: Society of Photo-Optical Instrumentation Engineers

Persistent URL: http://hdl.handle.net/1721.1/52622

Version: Final published version: final published article, as it appeared in a journal, conference proceedings, or other formally published context

Neural Network Microwave Precipitation Retrievals and Modeling Results

R. Vincent Leslie, William J. Blackwell, Laura J. Bickmeier, and Laura G. Jairam
MIT Lincoln Laboratory, 244 Wood St., Lexington, MA, USA

ABSTRACT

We describe a simulation methodology used to develop and validate precipitation retrieval algorithms for current and future passive microwave sounders with emphasis on the NPOESS (National Polar-orbiting Operational Environmental Satellite System) sensors. Precipitation algorithms are currently being developed for ATMS, MIS, and NAST-M. ATMS, like AMSU, will have channels near the oxygen bands throughout 50-60 GHz, the water vapor resonance band at 183.31 GHz, as well as several window channels. ATMS will offer improvements in radiometric and spatial resolution over the AMSU-A/B and MHS sensors currently flying on NASA (Aqua), NOAA (POES) and EUMETSAT (MetOp) satellites. The similarity of ATMS to AMSU-A/B will allow the AMSU-A/B precipitation algorithm developed by Chen and Staelin to be adapted for ATMS, and the improvements of ATMS over AMSU-A/B suggest that a superior precipitation retrieval algorithm can be developed for ATMS. Like the Chen and Staelin algorithm for AMSU-A/B, the algorithm for ATMS to be presented will also be based a statistics-based approach involving extensive signal processing and neural network estimation in contrast to traditional physics-based approaches. One potential advantage of a neural-network-based algorithm is computational speed. The main difference in applying the Chen-Staelin method to ATMS will consist of using the output of the most up-to-date simulation methodology instead of the ground-based weather radar and earlier versions of the simulation methodology.

We also present recent progress on the millimeter-wave radiance simulation methodology that is used to derive simulated global ground-truth data sets for the development of precipitation retrieval algorithms suitable for use on a global scale by spaceborne millimeter-wave spectrometers. The methodology utilizes the MM5 Cloud Resolving Model (CRM), at 1-km resolution, to generate atmospheric thermodynamic quantities (for example, humidity and hydrometeor profiles). These data are then input into a Radiative Transfer Algorithm (RTA) to simulate at-sensor millimeter-wave radiances at a variety of viewing geometries. The simulated radiances are filtered and resampled to match the sensor resolution and orientation.

1. INTRODUCTION

In this paper, we report on recent work to develop precipitation-rate retrieval algorithms for the next generation of passive microwave sensors on NPOESS (National Polar-orbiting Operational Environmental Satellite System). The NPOESS microwave sensors are the Advanced Technology Microwave Sounder (ATMS) and the Microwave Imager / Sounder (MIS). MIS replaces the defunct Conical-scanning Microwave Imager / Sounder (CMIS). ATMS scans cross-track, while MIS has a conical scan. ATMS and MIS have similar channel sets, but MIS has polarimetric capabilities and channels at C- and X-band. Heritage instruments for ATMS include AMSU, HSB, and MHS, and MIS has the Advanced Microwave Sounding Radiometer for the Earth Observing System (AMSR-E) and Tropical Rainfall Measurement

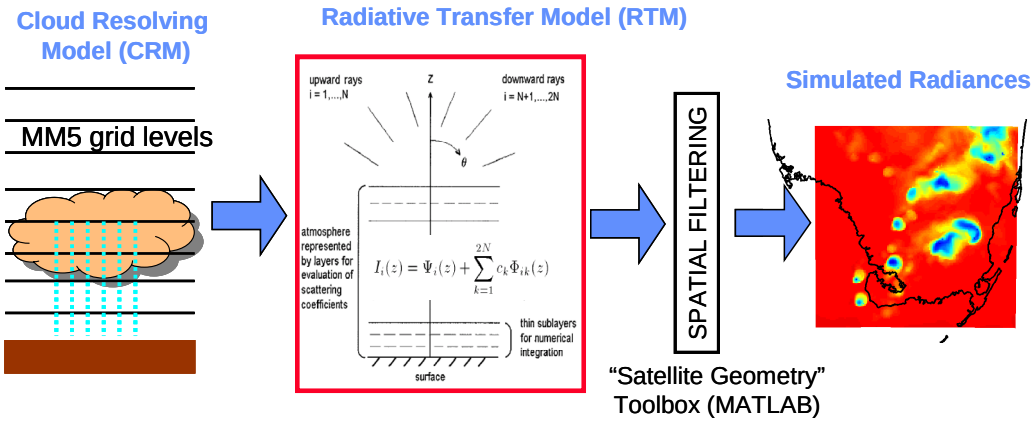

Fig. 1. Simulation methodology.

Microwave Remote Sensing of the Atmosphere and Environment VI, edited by Azita Valinia, Peter H. Hildebrand, Seiho Uratsuka, Proc. of SPIE Vol. 7154, 715406 · © 2008 SPIE · CCC code: 0277-786X/08/$18 · doi: 10.1117/12.804815

Mission (TRMM) Microwave Imager (TMI).

An important aspect of the retrieval algorithm is the development of a microwave radiance simulation methodology. The algorithm utilizes a data set of matched radiances with know rain rates. This is empirically difficult to collect; therefore, the simulation methodology allows the development of a simulated ensemble. We validate the methodology using the NPOESS Aircraft Sounder Testbed - Microwave (NAST-M) during the Cirrus Regional Study of Tropical Anvils and cirrus Layers – Florida Area Cirrus Experiment (CRYSTAL-FACE 2002) field campaign by comparing the simulated radiances with the aircraft measurements.

The precipitation retrieval technique utilizes a multi-layer feed-forward Neural Network (NN) that is trained using the radiance simulation methodology. NNs were trained for both the ATMS and MIS instruments. Presently, the training ensemble was developed with an early version of the simulation methodology.

Section 2 describes the simulation methodology, which includes the Cloud-Resolving Model (CRM), Radiative Transfer Algorithm (RTA), and satellite geometry toolbox. Section 3 discusses the validation of the methodology with an aircraft sensor, i.e., NAST-M. Sec. 4 describes the retrieval algorithm for the ATMS and MIS sensors. Sec. 5 gives a summary and future work.

2. SIMULATION METHODOLOGY

The CRM is used to generate the atmospheric state (e.g., hydrometeor profile). The RTA converts the atmospheric state from the CRM to a brightness temperature characterized by the target sensor's spectral and spatial characteristics. The CRM's native spatial resolution (~1 km) is convolved with the sensor's antenna pattern using a function in the Satellite Geometry Toolbox developed by F. W. Chen.

2.1 Cloud-resolving model

The CRM used is the Pennsylvania State University / National Center for Atmospheric Research Mesoscale Model, or MM5. MM5 can be run at the cloud-resolving scale of one kilometer, which allows the use of an explicit microphysics parameterization. These parameterizations simulate the hydrometeor profiles. The model has other pertinent outputs such as the temperature and humidity profiles.

TABLE I
CRYSTAL-FACE 2002 FIELD CAMPAIGN

Date	Weather [A]	CRM – MM5
03Jul02	CC	Simulated
07Jul02	CC, SF	Simulated
09Jul02	CC, SF	
11Jul02	CC	Simulated
13Jul02	CC	Simulated
17Jul02	SF	Simulated
19Jul02	CC	Simulated
21Jul02	CC	Simulated
23Jul02	CC	Simulated
29Jul02	SF	Simulated
30Jul02	SF	

[a] CC = convective cells, SF = stratiform precipitation

Table I lists the sorties that NAST-M collected data during CRYSTAL-FACE 2002. Each sortie has its own MM5 run. The run begins by defining three grids that cover the geographical area that the flight flew over. The outer grid has the coarsest resolution of nine km (72 x 72 pixels). The two other grids are nested inside, so each smaller grid is within the boundaries of the larger grid. The middle grid is 121 x 121 pixels (3 km apart), and the highest resolution grid is 241 x 241 pixels and spaced one km apart. This highest resolution grid is used to simulate aircraft radiances because the grid spacing is smaller than the antenna footprints (~2.5 km). MM5 used a 25-category USGS data set, with categories like grassland, mixed forest, etc., to give each grid point a vegetation type.

The simulations begin with a low-spatial-resolution initialization, which is typically the output of another mesoscale or global circulation model. Initialization data was collected for each of the sorties. Depending on availability, the initialization data's spatial resolution ranged from 40 to 32 km and was typically available in three hour intervals. They were the North American Regional Reanalysis (NARR), North American Mesoscale (NAM), or Rapid Update Cycle (RUC). Since the simulations were cold starts (i.e., there was no cloud information in the initialization data), the MM5 run began approximately three hours before the targeted precipitating event. The output of the MM5 was saved every 15 minutes. The MM5 runs did not use objective analysis (i.e., improving the initialization with observations, e.g., radiosondes) or other data assimilation (i.e., Four-Dimensional Data Assimilation) that drive the simulation to observations during the run. The runs did use the initialization data for boundary conditions that were interpolated between the initialization data's three hour intervals.

The comparison with NAST-M in Section 3 used the Reisner 2 microphysics model (also known as an explicit moisture scheme). The six phases of the scheme are rain, snow, graupel, cloud water, cloud ice, and water vapor. The retrieval technique in Sec. 4 used the Goddard microphysics option with graupel. Other MM5 physics options include

using the Grell cumulus parameterization for the 9-km grid, which models clouds that cannot be fully resolved by the explicit moisture schemes at such coarse resolutions. The soil model was the five-layer "slab" model, and the planetary boundary layer model used the Medium Range Forecast Model (MRF) option.

2.2 Radiative transfer algorithm

Once the atmospheric state is simulated with the CRM, the equation of radiative transfer allows the radiance of the airborne or spaceborne instrument to be simulated. The radiative transfer equation defines the physics of the thermal radiation between a source, an intervening medium, and a receiver. In this application, the source is the earth's surface and the intervening medium is the atmosphere. The atmosphere can be opaque or transparent depending on the absorption of the atmospheric constituents. The molecular constituents in the atmosphere, e.g., O_2, have different mechanisms to absorb incident electromagnetic energy. The microwave and far-infrared frequencies are mainly absorbed by the rotational transitions of the diatomic molecules. In thermal equilibrium, which is assumed for atmospheric parcels, the molecules will also emit electromagnetic energy in accordance to Planck's radiation law and will be a function of the molecular constituent's temperature. The upper left hand corner of Fig. 2 has the zenith opacity of the standard atmosphere and the passbands of the pertinent microwave instruments.

Two numerical solutions were used to solve the radiative transfer equation. The primary technique is called TBSCAT [1]. TBSCAT integrates an ensemble of trial functions. The trial functions are bounded at the top of the atmosphere with the downward-propagating radiances, and then surface boundary conditions are imposed after integration. If the atmosphere becomes opaque during the integration, then the integration ends and a special boundary condition is

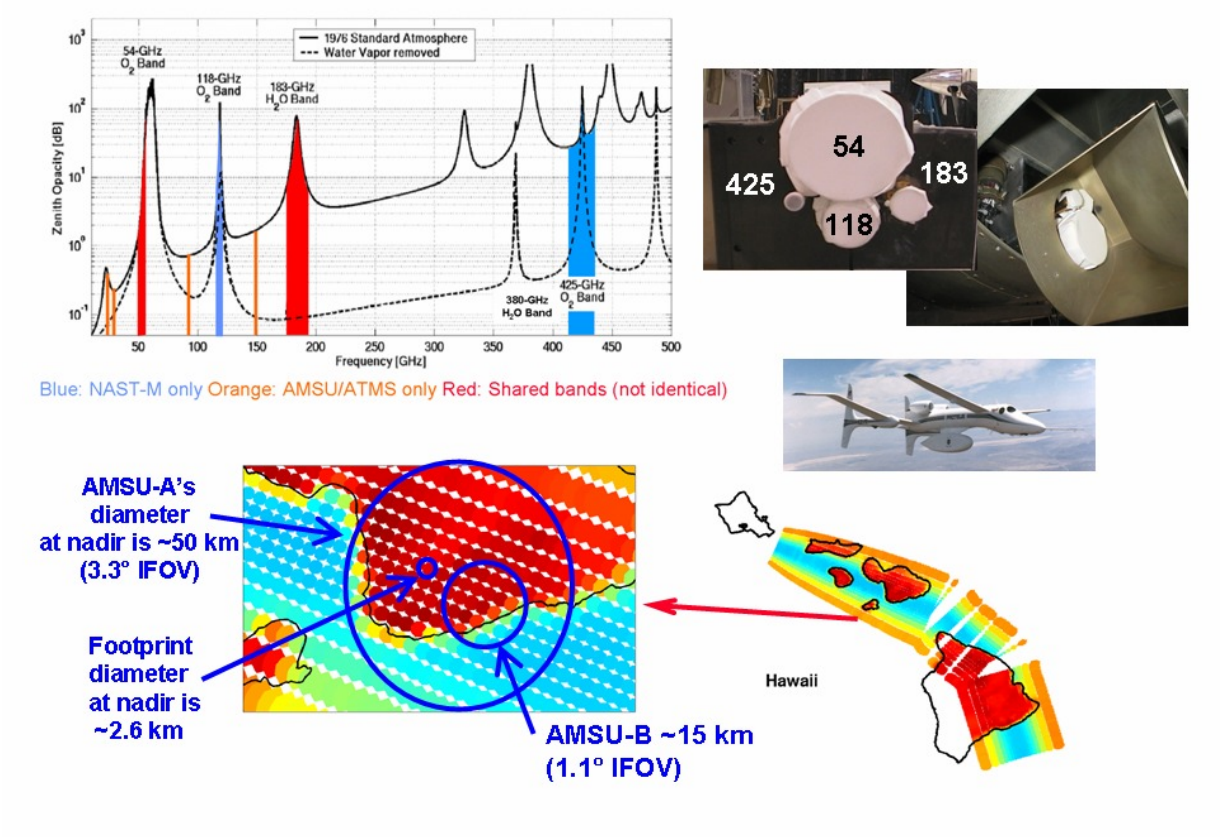

Fig. 2. NAST-M scanning assembly, zenith opacity, and sample data featuring various field of view.

imposed. TBSCAT trade studies were made between accuracy and computation efficiency, which determined that ten trial functions or "streams" gave the most accurate precipitating brightness temperatures. TBSCAT is fast algorithm, but can be numerically unstable at high rain rates using 10 streams. When the TBSCAT results were numerically unstable, the TBSOI [7] solution technique replaced the TBSCAT results. TBSOI uses the Successive Order of Interaction (SOI)

technique, which combines the doubling technique with successive-order-of-scattering (SOS) technique. TBSOI showed better stability at the higher rain rates.

The volumetric density (grams/cubic meters) of the various hydrometeor types (provided by the CRM) are separated by radius. The RTA models the hydrometeors as perfect spheres. The separation into radii bins follows literature standards for Drop-Size Distributions (DSD). Snow used the Sekhon-Srivastava DSD [2], while rain and graupel used the Marshall-Palmer DSD [3]. Typically, the SS-DSD is used with graupel, but better results were found with the MP-DSD. The intrinsic densities of the hydrometeor types were kept consistent with the literature and matched the values in the CRM. Snow, graupel, and rain are 0.1 g/cm^3, 0.4 g/cm^3, and 1.0 g/cm^3, respectively.

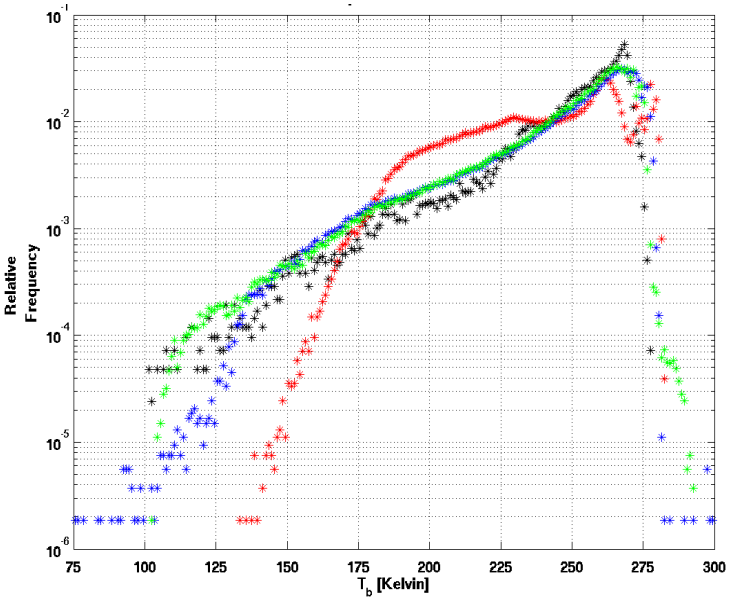

Fig. 3. Histogram of 118.75 ± 2.05 GHz with various RTAs. Only precipitating pixels are shown. Black are the actual NAST-M measurements (see text in Sec. 3.2).

The RTA was tailored to meet the spectral and spatial characteristics of the sensor. Antenna patterns were model as Gaussian and had 3-dB beamwidths that matched the actual sensors. The channels were modeled as impulses at the center frequencies of the channel's passband. Double-side band channels had two impulses that matched the center frequency of the upper and lower sideband. Based on the land category in the MM5 initialization (USGS), the emissivity of each pixel was calculated. If the category was "water bodies," then the water emissivity model, fastem [9], was used to calculate the microwave emissivity. Swamp and irrigated crops where simulated as 10% the value from fastem and the other 90% used an emissivity of 0.95. Land categories used a random emissivity that ranged between 0.90 and 0.98.

3. METHODOLOGY VALIDATION

The results of the simulation methodology, presented in Sec. 2, are validated in this section against measurements made with an airborne passive microwave sensor during field campaigns. The weather simulated using the CRM would not match the actual weather during the aircraft sortie because of the limitations of the initialization data and CRM. To compare the simulated and measured data, the brightness temperatures were compared in histograms. Furthermore, the histograms were normalized to allow a more appropriate comparison. Many simulated brightness temperature images were used in the histograms, and future work will attempt to segregate images to try to better match weather phenomenon.

3.1 Airborne microwave sensor

The NAST-M instrument suite [4],[5] includes a total of four spectrometers, with three operating near the oxygen lines at 50–57, 118.75, and 424.76 GHz, and a fourth spectrometer centered on the water vapor absorption line at 183.31 GHz. The NAST-M 54-GHz spectrometer has five channels matching corresponding AMSU-A channels, and the 183-GHz spectrometer has three channels matching corresponding AMSU-B and MHS channels. All four of NAST-M's feedhorns are co-located, and have 3-dB (full-width at half-maximum) beamwidths of 7.5°, which translates to approximately 2.5-km nominal pixel diameter at nadir incidence. The four feedhorns are directed at a single mirror that scans cross-track beneath the aircraft, spanning ± 65 degrees. The NAST-M sensor package is mounted on an aircraft platform with a typical cruising altitude of 17-20 km, which results in a nominal swath width of 100 km. Fig. 2 shows pictures of NAST-M's scanning assembly and feedhorns. Also included is the zenith opacity of the standard atmosphere along the microwave spectrum with important passbands marked out. The bottom of the figure shows an illustration of the measured radiances projected onto the earth's surface using Mathwork's MATLAB software. The 50-GHz window channel is shown and AMSU IFOVs are marked for reference.

3.2 Histogram validation

Due to the difficulty of accurately simulating the weather conditions, i.e., the simulations won't spatially and temporally match the NAST-M radiances measured during the CRYSTAL-FACE 2002 sorties, the radiances have to be compared using histograms.

Fig. 3 is an example of a single NAST-M channel, and it illustrates the progression of the RTA development to accurately match the NAST-M measurements. The radiances are in one Kelvin bins (abscissa), and the ordinate is the relative frequency inside that bin. The baseline is the NAST-M measurements, which are the black asterisks (41,670 precipitating measurements). The technique in [8] was used to identify precipitating NAST-M pixels. The other three colors represent simulated radiances with different variations of the RTA. The simulations totaled the equivalent of 535,126 precipitating measurements. The red asterisks are the work of Surussavadee and Staelin [6], which utilized a two-stream version of TBSCAT and a tuned intrinsic density of the hydrometeors. The blue asterisks used a ten-stream version of TBSCAT and the common literature values of the intrinsic densities. The last version, green asterisks, used

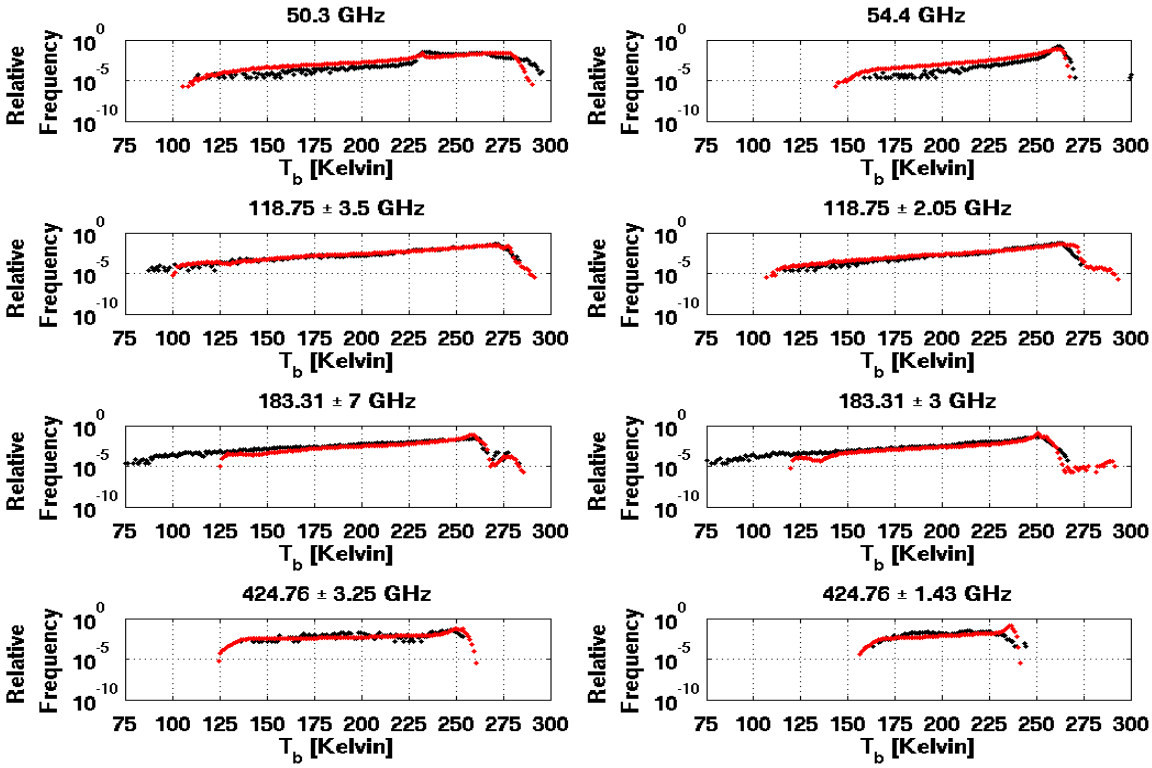

Fig. 4. Comparison between NAST-M measurements during CRYSTAL-FACE 2002 and simulated radiances derived from a cloud-resolving model. Only precipitating pixels were used in the histograms.

the TBSCAT from the blue version, but when TBSCAT identified a possible numerical instability in the radiative transfer solution, TBSOI [7] was used to recalculate the radiance.

To give a more comprehensive comparison, select NAST-M channels are presented in Fig. 4. The black dots are the NAST-M observations and the red dots are the simulated brightness temperatures (Tb) using the RTA from the green asterisks described in Fig. 3. The coldest Tb are the heaviest precipitation (left hand side of the histogram), and the warmest are light precipitation. The discrepancies at the warmest Tb is attributed to the difficulty of identifying precipitating pixels from the NAST-M data (black asterisks) and simulations that still have numerical instability (red asterisks), e.g., 183-GHz channels. Further work must be done in regards to the 183-GHz channels to provide stable and accurate Tb at the highest precipitation rates.

4. PRECIPITATION RETRIEVALS

The development of a NPOESS microwave precipitation-rate retrieval algorithm will draw upon lessons learned from the AMSU algorithm described in [8].

4.1 Satellite instruments

The NPP and some NPOESS satellites will be equipped with the ATMS, which will have additional channels and better resolution and sampling than its predecessors such as the AMSU-A/B on NOAA-15, NOAA-16, and NOAA-17; the AMSU/HSB on Aqua; and the AMSU-A/MHS on NOAA-18 and METOP-A. The spectral differences consist of ATMS having additional channels at 51.76, 183.31±1.8, and 183.31±4.5 GHz. Also, the 157-GHz channel on MHS is replaced by a 165±0.925-GHz channel on ATMS. Lastly, the single-sideband 190.31-GHz channel on MHS is replaced by a 183.31±7.0-GHz channel.

On AMSU, the sounding and lower moisture-viewing channels (23.8 to 57.29 GHz) have a 3.3° beamwidth that results in a ~50 km diameter footprint at nadir. Conversely, the ATMS lower moisture channels (23.8 and 31.4 GHz) have a 5.2° beamwidth and a ~75-km footprint at nadir. The ATMS temperature sounding channels (50.3 to 57.29 GHz) have a 2.2° beamwidth and a ~32-km footprint at nadir. The humidity profiling channels on AMSU-B/MHS (157-190.31 GHz) and ATMS (166 to 183.31±7.0 GHz) have a beamwidth of 1.1°, which results in a footprint diameter of ~16 km at nadir. The 89-GHz channels on AMSU have resolutions of both 1.1° and 3.3°. This channel is used to gain information on surface temperature and emissivity, and to detect precipitating or cloudy pixels. The similar channel on ATMS is at 88.2 GHz with a beamwidth of 2.2°. AMSU does not have spatial oversampling, while the 5.2° and 2.2° spatial resolutions on ATMS will be oversampled.

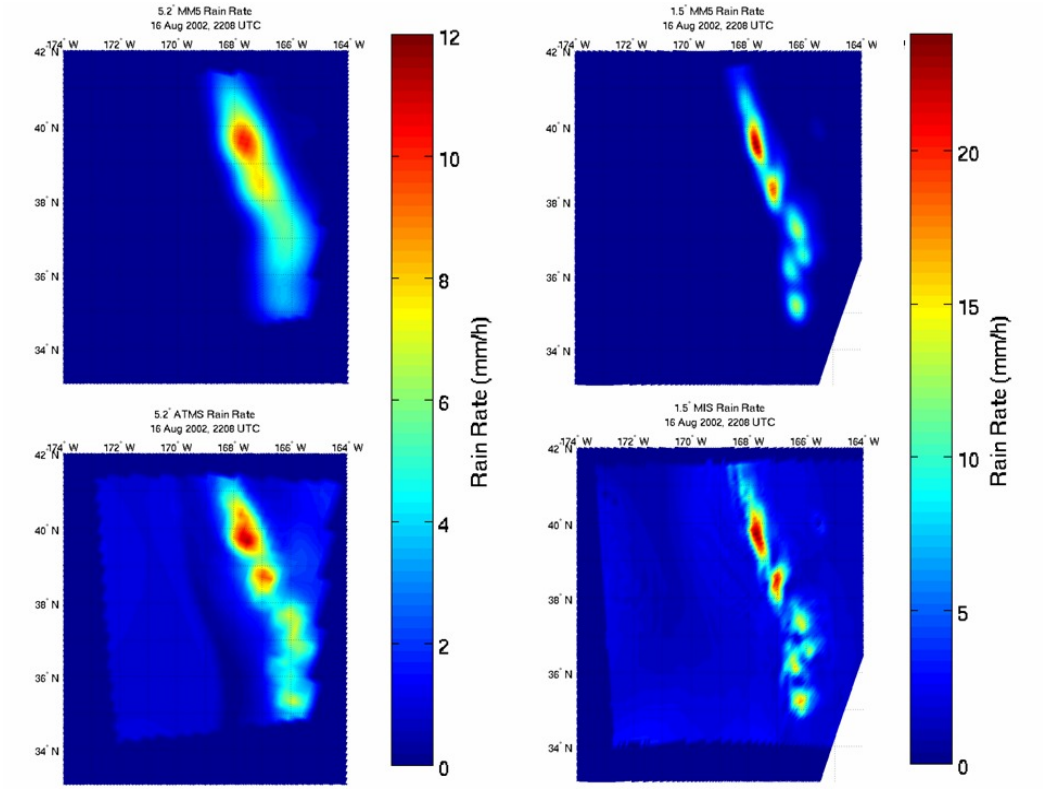

Fig. 5. Top two figures are the MM5 output's surface rain rate filtered to 5.2° and 1.5° resolution to match ATMS and MIS, respectively. The bottom two figures are the corresponding output of the best neural network. (Left hand side: ATMS; Right hand side: MIS)

MIS is a conically scanning sensor as compared to the cross-track scanning AMSU and ATMS. Therefore the MIS has a fixed Earth incident angle ~55°. The beamwidths range from 1.5° for the 6.8-GHz, 1.0° for 10.7 GHz, 0.6° for 18.7 and 23.8 GHz, 0.41 for 37 GHz, and 0.35° for the atmospheric and humidity sounding channels. These give an IFOV on the surface of ~45 km x 80 km at 6.8 GHz (cross track x along track). The temperature and humidity sounding has a

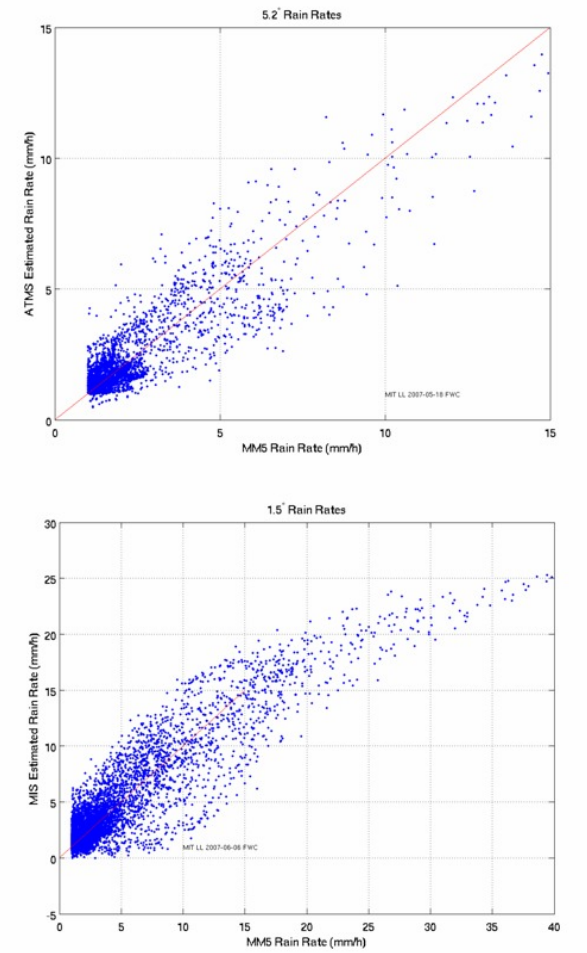

Fig. 6. Presented is the precipitation retrieval performance for the best ATMS and MIS neural networks. ATMS is on top and the MIS is on the bottom.

footprint of ~8 km x 14 km.

4.2 Retrieval methodology

For this study, a simple NN estimator was trained to estimate MM5 rain rate that was filtered to 5.2° or 1.5° resolution (see top two images in Fig. 5). The 5.2° data was used to train the ATMS NNs because the 23.8-GHz and 31.4-GHz channels have the coarsest resolution of 5.2°. A similar situation exists for MIS, because MIS's coarsest resolution comes from the 6-GHz channels at 1.5°. The Earth incident angle was at 47° during these preliminary studies. The ATMS algorithm used all 22 ATMS channels, and the MIS algorithm used 18 tentative channels. The NNs had one hidden layer with up to ten tangent sigmoid nodes and an output layer with one linear node.

Data for the training, validation, and testing sets were collected from data sets consisting of 25 examples of oceanic precipitation between July and December 2002. This gave 10,983 ATMS pixels and 56,300 MIS pixels. The pixels collected were divided evenly among the training, validation, and testing sets. Pixels where the filtered MM5 rain rate was less than 1 mm/hr were excluded. The training set was used to adjust the weights during training, the validation set was used to determine when training should stop, and the testing set was used to evaluate the performance of the NN. The bottom two images in Fig. 5 are examples of the output of the best performing NN. The matching MM5 "truth" is in the top two images. The ATMS NNs also included satellite zenith angle as an input. Ten NNs were initialized using the Nguyen-Widrow method and trained using the Levenberg-Marquardt method, where the best performing NN was kept. Each net was trained for up to 100 epochs.

4.3 Performance evaluation

Fig. 6 compares outputs of the NN with the best performance over the testing set with the MM5 surface rain rates. The RMS error of the best ATMS NN was 0.83 mm/h and the best MIS NN gave 1.42 mm/h over the rain rate range of 1-15 mm/h.

5. SUMMARY AND FUTURE WORK

The fundamental building blocks are in place for a complete precipitation retrieval system. Recent studies highlight the need for accurate radiative transfer modeling in regions of heavy precipitation. AMSU experience and preliminary studies show ATMS and MIS can provide accurate, high-resolution, global precipitation products. Future work will focus on the CRM data generation, continued RTA validation, and retrieval algorithm optimization. Some of the retrieval algorithm optimizations will be to utilize some of the signal processing methods in the Chen-Staelin algorithm for AMSU-A/B, which are regional Laplacian interpolation for cloud flagging, principal component analysis for temperature profile characterization, and image sharpening (enables retrievals at the finest resolution possible).

6. ACKNOWLEDGMENTS

This work was supported through the NPOESS Integrated Program Office Internal Government Studies Program. The authors would also like to thank Frederick W. Chen for his work on the precipitation retrieval algorithm. This work was

sponsored by the National Oceanographic and Atmospheric Administration under Air Force Contract FA8721-05-C-0002. Opinions, interpretations, conclusions, and recommendations are those of the authors and are not necessarily endorsed by the United States Government.

REFERENCES

[1] P. W. Rosenkranz, "Radiative Transfer Solution Using Initial Values in a Scattering and Absorbing Atmosphere With Surface Reflection," IEEE Trans. Geosci. Remote Sensing, 40, 1889-1892 (2002).
[2] R. S. Sekhon and R. C. Srivastava, "Snow Spectra and Radar Reflectivity," J. Atmos. Sci., 27, 299-307 (1970).
[3] J. S. Marshall and W. McK. Palmer, "The distribution of raindrops with size," Journal of Meteorology, 5, 165-166 (1948).
[4] W. J. Blackwell *et. al*, "NPOESS Aircraft Sounder Testbed-Microwave (NAST-M): Instrument description and initial flight results," IEEE Trans. Geosci. Remote Sensing, 39, 2444-2453 (2001).
[5] R. V. Leslie and D. H. Staelin, "NPOESS Aircraft Sounder Testbed-Microwave: Observations of Clouds and Precipitation at 54, 118, 183, and 425 GHz," IEEE Trans. Geosci. Remote Sensing, 42, 2240-2247 (2004).
[6] C. Surussavadee and D. H. Staelin, "Comparison of AMSU Millimeter-Wave Satellite Observations, MM5/TBSCAT Predicted Radiances, and Electromagnetic Models for Hydrometeors," IEEE Trans. Geosci. Remote Sensing, 40(8), 2667-2678 (2006).
[7] A. K. Heidinger, C. O'Dell, R. Bennartz, and T. Greenwald, "The Successive-Order-of-Integration Radiative Transfer Model. Part I: Model Development," J. Appl. Meteor. Climatol., 45, 1388-1402 (2006).
[8] F. W. Chen and D. H. Staelin, "AIRS/AMSU/HSB Precipitation Estimates," IEEE Trans. Geosci. Remote Sensing, 41(21), 410-417 (2003)
[9] S. J. English and T. J. Hewison, "A fast generic millimetre-wave emissivity model," In Proceedings of SPIE, 3503, 288-300 (1998).